J Therm Anal Calorim (2012) 107:85–96
DOI 10.1007/s10973-011-1686-3

Thermal stability and UV-shielding properties of polymethyl methacrylate and polystyrene modified with calcium carbonate nanoparticles

Manoj Kumar Pal · Beena Singh · Jaiswar Gautam

29th STAC-ICC Conference Special Chapter

Abstract The influences of nanosized $CaCO_3$ on the thermal and optical properties embedded in poly(methyl methacrylate) (PMMA) and polystyrene (PS) were investigated. Calcium carbonate nanoparticles were synthesized by in situ deposition technique, and its nano size (32–35 nm) was confirmed by scanning electron microscope (SEM) and X-ray studies. Nanocomposites samples of PMMA/$CaCO_3$ and PS/$CaCO_3$ were prepared with different filler loading (0–4 wt%) of $CaCO_3$ nanoparticles by solution mixing technique. The Fourier transform infrared analysis confirmed that $CaCO_3$ nanoparticles were present in the polymers matrices. The morphology and elemental composition of nanocomposites were evaluated by SEM and energy dispersive X-ray spectroscopy. The thermal properties of nanocomposites were characterized by differential scanning calorimetric, thermogravimetric, and differential thermogravimetry analysis, and the results indicate that the incorporation of $CaCO_3$ nanoparticles could significantly improve the thermal properties of PMMA/$CaCO_3$ and PS/$CaCO_3$ nanocomposites. The glass transition temperature (T_g) and decomposition temperature (T_d) of nanocomposites with 4 wt% of $CaCO_3$ nanoparticles were increased by 30 and 24 K in case of PMMA/$CaCO_3$ and 32 and 15 K in the case of PS/$CaCO_3$ nanocomposites, respectively. The obtained transparent nanocomposites films were characterized using UV–Vis spectrophotometer which shows the transparencies of nanocomposites are almost maintained in visible region while the intensity of absorption band in ultraviolet (UV) region is increased with $CaCO_3$ nanoparticles contents and these composites particles could enhance the UV-shielding properties of polymers.

Keywords $CaCO_3$ nanoparticles · PMMA · PS · SEM–EDS · TG/DTG · UV–Vis shielding

M. K. Pal · B. Singh · J. Gautam (✉)
Department of Chemistry, Dr. B. R. Ambedkar University, Agra 282002, India
e-mail: gjaiswar@gmail.com

M. K. Pal
e-mail: manojkumarpal3@gmail.com

B. Singh
e-mail: bnsingh65@gmail.com

Introduction

Nanoinorganic as additives into polymer system has resulted in polymer nanocomposites exhibiting multifunctional, higher performance polymer characteristics beyond what traditional filled polymeric material possess. Multifunctional feature attributable to polymer nanocomposites consist of improved thermal resistance and/or flame resistance, ultraviolet (UV) protection, mechanical properties, acid resistance, rheological properties, moisture resistance, decreased permeability, change dissipation, chemical resistance etc. [1–7]. Through control/alteration of the additives at the nanoscale, one is able to maximize preparation enhancement of selected polymer system to meet or exceed the requirement of current military, aerospace, and commercial application [8].

Various nanoscale fillers, including montmorillonite, silica, calcium carbonate, zinc oxide, aluminum oxide, etc. reported to enhance the thermal, mechanical, and optical properties. Nanosized calcium carbonate ($CaCO_3$) is one of the most common inorganic nanofillers used in the preparation of nanocomposites, and it has been widely used as fillers in the areas of plastics, rubbers, paints, papermaking, textiles, pigments, ceramics, medicine, pharmacy, and so on, in virtue of its different physical and chemical

properties and many of its important technological applications [9–13]. During the past years, many studies have been done on the elaboration of nanocomposites system by embedding of calcium carbonate nanoparticles into polymeric matrix [14–16], affording a new class of polymeric materials which combine the properties of inorganic particles with the processability and flexibility of organic polymer matrix.

Inorganic–polymer nanocomposites, which exhibit an ensemble of properties of both inorganic nanoparticles and polymers, are excellent materials for UV-shielding applications. Such composites benefit from physical flexibility and ease of processing, which are typical characteristics of polymers. The optical absorption spectrum is one of the most important tools for understanding band structure and electronic properties of pure and filled polymers. This technique depends on the transition of some electrons from the valence band (VB) to the conduction band (CB), when photon energy is greater than the band energy. As a consequence, the nanocomposites properties are strongly influenced by the nature of the interface between the inorganic nanoparticles, and the polymer matrix can give rise to some unusual properties in these materials [17, 18].

Poly(methylmethacrylate) (PMMA) and polystyrene (PS) are well known for their good optical and chemical properties. Some researchers have reported the incorporation of ZnO, SiO_2, or TiO_2 nanoparticles into PMMA or PS matrices, respectively to fabricate the transparent nanocomposites film [19–23]. On the other hand, PMMA and PS are the important technopolymer finding application in many sectors such as aircraft glazing, signs, lighting, architecture, transportation, engineering, and high-performance products. The effects of $CaCO_3$ nanoparticles on the thermal, mechanical, acid-resistance, optical etc. properties of PMMA and PS have been reported [7, 24–27]. Elimat et al. [27] indicated that the thermal conductivity of pure PMMA increased with addition of 2 wt% $CaCO_3$ nanofiller and in optical properties the Urbach tail for pure PMMA is less than that for PMMA/$CaCO_3$ composite. Ma et al. [25] found that increase the loading of $CaCO_3$ in the composites can improve the thermal stability of PMMA and the acid resistance of $CaCO_3$ nanoparticles in composites. Zeng et al. [28] prepared highly transparent ZnO/PMMA–PS nanocomposites film by effective solution mixing method, and the film could block the UV radiation up to 97% and allow 98% of visible light to pass through with 2 wt% ZnO in the matrix. Tu et al. [29] developed a solution casting approach to obtaine ZnO/PS nanocomposites film which exhibits excellent thermal and UV-absorbing properties than pure polystyrene.

This study is part of a systematic study of the effect of the addition of nanofiller into polymer matrix for the purpose of characterizing thermal and UV-shielding properties of PMMA/$CaCO_3$ and PS/$CaCO_3$ nanocomposites. The nanoparticles and nanocomposites were characterized by evaluating their chemical composition through Fourier transform infrared (FT-IR) spectroscopy, crystallinity, and particles size of nanoparticles by XRD, their shape, size, and distribution in polymer matrix with elemental composition by scanning electron microscope–energy dispersive X-ray spectroscopy (SEM–EDS). On the other hand, the influences of $CaCO_3$ nanoparticles on the glass transition temperature, as well as on the decomposition temperature of the PMMA and PS matrix were studied in detailed by differential scanning calorimetric (DSC), thermogravimetric (TG), differential thermogravimetry (DTG) analysis. UV–Vis absorbance spectra were evaluated by UV–Vis double beam spectrophotometer. In our study, an attempts were made to demonstrate the thermal stability and UV-protection of polymers that can be achieved by incorporation of $CaCO_3$ nanoparticles into PMMA and PS matrices.

Experimental

Materials used

For the preparation of calcium carbonate nanoparticles, analytical graded calcium chloride ($CaCl_2$), potassium carbonate (K_2CO_3), and poly(ethylene glycol) (PEG, MW = 6000) were procured from Merck, India. Stabilized methyl methacrylate (MMA) and styrene were obtained from Alfa Aeasar, Germany. Monomers were washed three times by 10% NaOH solution to remove inhibitors and were kept in cool and dry place. Benzoyl peroxide (BPO) supplied by CDH, Laboratory reagent, India, was used after recrystallized from methanol. Organic solvents like methyl alcohol, toluene, benzene, chloroform, acetone etc. were used after double distillation.

Nanoparticles synthesis and nanocomposites formation

The nanoparticles of calcium carbonate were synthesized by in situ deposition technique which was carried out in same manure as reported earlier [30]. Calcium chloride (11.1 g, 0.1 M) was dissolved in double distilled water (100 mL), whereas PEG (37.2 g, 0.0062 M) separately dissolved in hot double distilled water (100 mL). These solutions were mixed properly by stirring and digested gently for 12 h. Then solution of potassium carbonate (10.6 g, 0.1 M) was then added slowly with stirring. This solution was allowed to digest overnight, and finally the nanoparticles were filtered, washed thoroughly with double distilled water, till freed from PEG traces, and then dried at 383 K for 2 h. The filler was heated at about 523 K for removing traces of moisture before compounding.

In order to prepare PMMA/$CaCO_3$ and PS/$CaCO_3$ nanocomposites following steps have been taken to prepare nanocomposites samples:

1. Appropriate ratio of $CaCO_3$ nanoparticles were taken in 25 ml of chloroform, and the solution was magnetically stirred for 30 min at 343 K. Whitish coloured solution was obtained.
2. The PMMA and PS were dissolved separately in 100 mL of chloroform. The solution was kept at 343 K in magnetic stirrer for 30 min till transparent homogenous solution of polymers was obtained, respectively.
3. To prepare composites solution, the $CaCO_3$ nanoparticles solution was added drop by drop into the polymers solution, and the obtained solution was also stirred for 30 min for homogenously dispersion of nanoparticles into the polymer matrix.
4. The solution casting method was adopted for the preparation of thin layer nanocomposites film which was casted on optical glass substrate and dried at 353 K for 4 h. Finally, all the samples were thermally treated at 373 K for 10 h under vacuum.

After evaporation of the solvent whitish-colored transparent films with thickness of about 25 μm were obtained (Table 1).

Characterization of nanoparticles and nanocomposites

The chemical structure of the synthesized $CaCO_3$ nanoparticles, PMMA/$CaCO_3$, and PS/$CaCO_3$ nanocomposites were analyzed by FT-IR spectroscopy with Thermo Nicolet, Avatar 370, HATR assembled instrument. The crystal phase and particles size of the synthesized nanoparticles were detected by XRD analysis with a Bruker AXS D8 Advance XRD instrument using Cu Kα ($\lambda = 0.15406$ nm) radiation under the accelerating voltage 40 kV current 35 mA and scanning rate 0.020°/s (scan range $2\theta = 3°-70°$). The SEM analysis of nanoparticles and its distribution in PMMA and PS matrix was done by JEOL Model JSM—6390LV SEM instrument. The detection of elemental composition of nanoparticles and nanocomposites were carried out by EDS with JEOL Model JED–2300 instrument. UV–Vis absorption spectra of nanocomposites in chloroform were obtained using a Systronics Double Beam Spectrophotometer 2201. Thermal stability of the pure polymers and composites was determined by TG and DTG analysis under flowing N_2 (80 mL min^{-1}) and a heating rate of 293 K min^{-1}. The test was performed on Perkin Elmer Diamond TG/DTA instrument. The glass transition temperatures of pure polymers and nanocomposites were characterized by DSC (Netzsch DSC 204). All measurements on DSC were performed using instrument in the temperature range from 303 to 473 K under nitrogen atmosphere (heating rate 283 K min^{-1}).

Table 1 Composition and sample code of PMMA/$CaCO_3$ and PS/$CaCO_3$ nanocomposites used in this investigation

PMMA/$CaCO_3$ (wt%)	0	1	2	4
Sample code	PMMAO	PMMA1	PMMA2	PMMA4
PS/$CaCO_3$ (wt%)	0	1	2	4
Sample code	PSO	PS1	PS2	PS4

Results and discussion

XRD characterization of $CaCO_3$ nanoparticles

Figure 1 showed the diffractograms of $CaCO_3$ nanoparticles for evaluation of particles diameter. For $CaCO_3$ nanoparticles, the diffraction peaks were observed at 2θ values of 29.399°, 35.996°, 39.426°, and 48.510° which corresponded to $CaCO_3$ crystal as calcite. All the peak positions were basically consistent with standard data for $CaCO_3$ structure (JCPDS card No. 47-1743). The results demonstrated that the sample was pure phase nanoparticles of $CaCO_3$ that shows high magnification peak at diffraction angle of 29.39° [31]. The full width at half maximum (FWHM) was measured, and particle size was calculated using the Debye–Scherrer's formula:

$$D = 0.9\lambda/\beta\cos\theta$$

where λ = wavelength of X-ray (0.1541 nm), β = FWHM (0.239°, 0.255°, 0.240°, and 0.269°), θ = diffraction angle in radian and D = particles diameter. The sample powder has an average particles diameter 33 nm.

FT-IR spectra of $CaCO_3$ nanoparticles, PMMA/$CaCO_3$, and PS/$CaCO_3$ nanocomposites

In the FT-IR spectra of calcium carbonate nanoparticles of calcite forms show strong absorption bands at 1490, 875, and 712 cm^{-1}. These bands were attributable to the vibration of carbon–oxygen double bond in the carbonate ion, and the corresponding FT-IR spectra show sharp bands at 875 and 712 cm^{-1} which is the characteristics of calcite [32] (Fig. 2).

In the FT-IR spectra of PMMA/$CaCO_3$ nanocomposites (Fig. 3), the bands at 2994 and 2952 cm^{-1} are due to CH_2 and CH_3 stretching vibrations of PMMA, respectively. A band at 1723 cm^{-1} appeared due to the presence of ester carbonyl group stretching vibration of PMMA. Bands at 1274 and 1150 cm^{-1} can be explained owing to the C–O (ester bond) stretching vibration. Bands at 992 and 751 cm^{-1} are due to the bending of C–H bond. The bands at 1490, 875, and 710 cm^{-1} in PMMA/$CaCO_3$ nanocomposites show the dispersion of $CaCO_3$ as calcite form in the

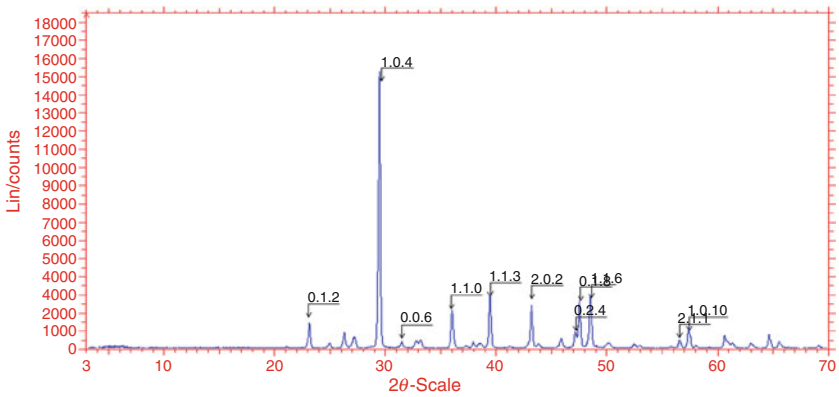

Fig. 1 XRD patterns of $CaCO_3$ nanoparticles

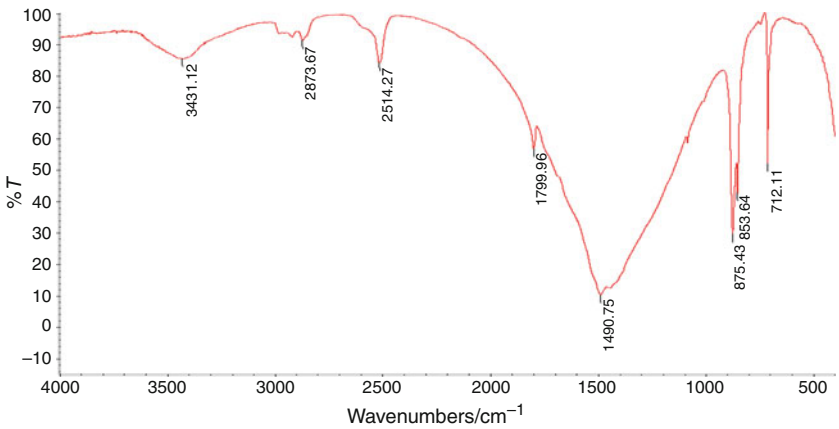

Fig. 2 FT-IR spectra of $CaCO_3$ nanoparticles

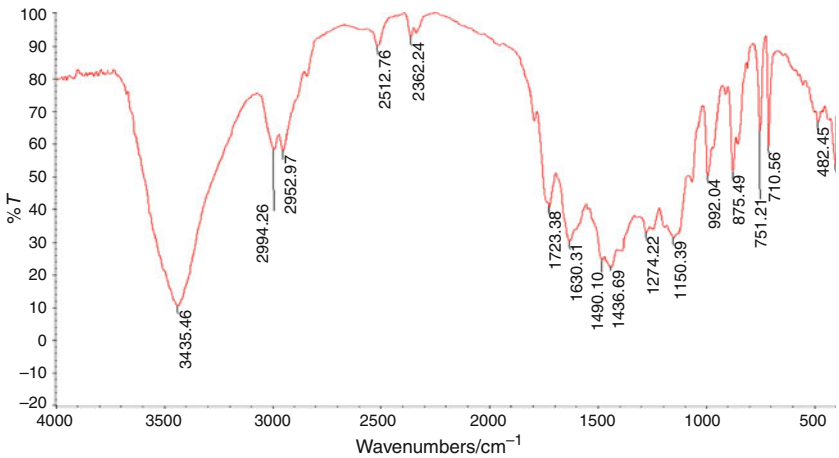

Fig. 3 FT-IR spectra of PMMA/$CaCO_3$ nanocomposites (PMMA2)

PMMA matrix. These bands can be also seen in PS/$CaCO_3$ nanocomposites (Fig. 4) for the incorporated $CaCO_3$ nanoparticles in the PS matrix, and the all characteristics bands of polystyrene like band for C–H aromatic stretching vibration at 3082 cm^{-1}, the C–H stretching vibration at 2942 cm^{-1}, and phenyl ring vibration at 1607, 1455, 755, and 697 cm^{-1} are clearly observed in this nanocomposite. These results clearly indicate that $CaCO_3$ nanoparticles are present in both polymer matrices (Table 2).

Morphology and elemental detection of the $CaCO_3$ nanoparticles, PMMA/$CaCO_3$, and PS/$CaCO_3$ nanocomposites

Figure 5 represents SEM micrograph and EDS graph of the nanoparticles and nanocomposites. Pure $CaCO_3$ nanoparticles can be clearly seen with cubic-like shape which is typically of calcite crystal of nearly equal dimension in the range of 30–35 nm. In order to evaluate the dispersion of

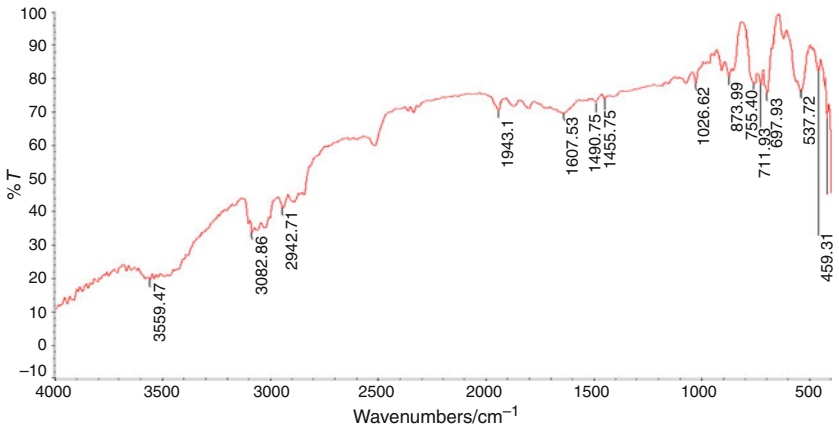

Fig. 4 FT-IR spectra of PS/$CaCO_3$ nanocomposites (PS2)

Table 2 FT-IR spectroscopic data of $CaCO_3$ nanoparticles, PMMA/$CaCO_3$ nanocomposites (PMMA2), and PS/$CaCO_3$ nanocomposites (PS2)

	Wave number (cm^1)	Group	Assignment
$CaCO_3$ nanoparticles	1490, 875, 712	C=O bond in the carbonate ion	υ(–C–O)
PMMA/$CaCO_3$ nanocomposites	2994, 2952	CH_3–, –CH_2–	υ(–C–H)
	1723	C=O (carbonyl)	υ(–C–O)
	1274, 1150	C–O (ester bond)	υ(–C–O)
	992, 751	CH_3–, –CH_2–	δ(–C–H)
	1490, 875, 710	C=O (Carbonate ion)	υ(–C–O)
PS/$CaCO_3$	3082	>CH– (aromatic)	υ(–C–H)
nanocomposites	2942	–CH_2–, >CH–	υ(–C–H)
	1607, 1455	–CH=CH– (phenyl ring)	υ(–C=C)
	1026	–CH=CH– (phenyl ring)	δ(-C–H)
	755, 697	–CH=CH– (phenyl ring)	δ(–C–H) out of plane
	1490, 873, 711	C=O (Carbonate ion)	υ(–C–O)

υ stretching vibrations, δ bending vibrations

$CaCO_3$ nanoparticles in the PMMA and PS matrix, the SEM were recorded for PMMA/$CaCO_3$ and PS/$CaCO_3$ (2 wt%) nanocomposites.

These SEM micrographs confirmed the good dispersion of $CaCO_3$ nanoparticles in the polymers matrices. EDS graph of Counts versus KeV shows that the percentage of calcium particles in the nanopowder was 9.60 with respect to other particles (Fig. 5a). The calcium percentage peak found in the nanocomposites was not same as in nanoparticles graph, the reason behind this that the less intense of the particles counts in the Fig. 5b, c may be due to $CaCO_3$ nanoparticles deeply dispersed in the polymer matrices as revealed from SEM micrograph which causes hard to remove the calcium electrons from the surface of polymer nanocomposites films. While increase in carbon peak in polymer nanocomposites shows a good adhesion between the surface of $CaCO_3$ nanoparticles and polymer matrices.

Thermal properties

Glass transition behavior

DSC curve of PMMA/$CaCO_3$ and PS/$CaCO_3$ nanocomposites with different $CaCO_3$ nanoparticles contents are shown in Fig. 6, and the glass transition temperatures (T_g's, (exothermic peak)) were listed in Table 3. The glass transition temperatures of pure PMMA and PS in nanocomposites increase with $CaCO_3$ nanoparticles contents which were directly related to the polymers chain mobility. It was found that the T_g of PMMA/$CaCO_3$ nanocomposites was higher than PS/$CaCO_3$ nanocomposites, but the percentage increasing of T_g was more in PS-based nanocomposites than PMMA-based nanocomposites. As revealed from FT-IR and SEM–EDS analysis, there was good interaction of nanoparticles and polymer matrix so due to this confinement of the polymer chain within the nanoparticles with restriction

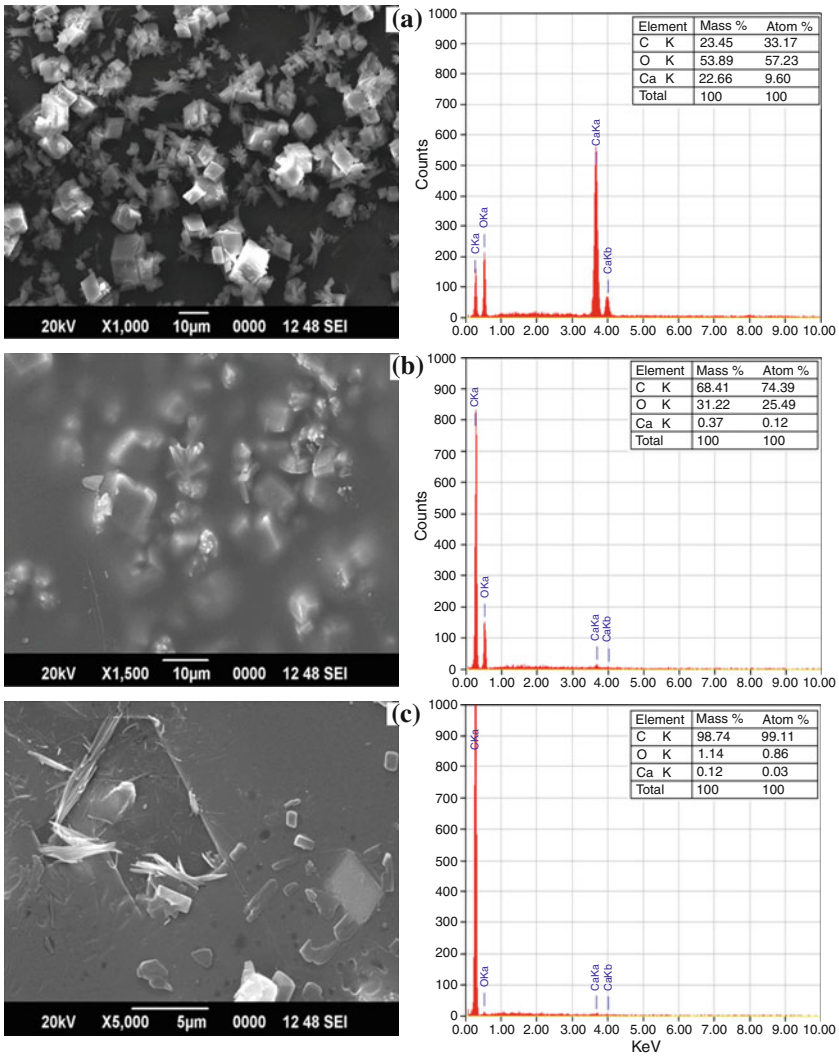

Fig. 5 SEM micrograph and EDS spectra of **a** $CaCO_3$ nanoparticles, **b** PMMA/$CaCO_3$, and **c** PS/$CaCO_3$ nanocomposites

Table 3 T_g's of PMMA/$CaCO_3$ and PS/$CaCO_3$ nanocomposites with 0–4 wt% loading of $CaCO_3$ nanoparticles

Fillers (%)	T_g of PMMA/$CaCO_3$ nanocomposites (K)	T_g of PS/$CaCO_3$ nanocomposites (K)
0	348.9	339.2
1	350.1	353.6
2	376.7	369.1
4	379.0	371.5

in the mobility of polymer chains and also due to agglomeration of nanoparticles at higher amount of $CaCO_3$ nanoparticles. This region in the vicinity of the polymer matrix evidently exhibits a dominant effect on the average glass transition temperature of composites, leading to the increase in the effective T_g due to the interaction with nanofillers and formation of nanophases. This behavior was similar to that observed in polycarbonate [33], polybutadiene rubber (PBR) [15], poly (vinyl chloride) [30]-based nanocomposite containing different nanofillers.

Thermal gravimetric analysis

The TG and DTG curve obtained in nitrogen atmosphere for pure polymers (PMMA and PS) and nanocomposites were shown in Figs. 7, 8, 9, 10, 11, 12, 13, and 14. The TG/DTG curve of pure PMMA and PS have strong peak at 651 and 693 K, respectively, suggesting that random chain scission is the main step during the polymer degradation process. In PMMA/$CaCO_3$ nanocomposites by loading 1, 2, and 4 wt% of $CaCO_3$ nanoparticles, the decomposition temperature (T_d) are 653, 660, and 675 K observed while in case of PS/$CaCO_3$ nanocomposites these temperatures were 696, 700, and 708 K that show an increase of $CaCO_3$ nanoparticles content, the T_d shifted toward higher values. The total weight-losing ratio of pure PMMA and PS was much higher than that of its corresponding nanocomposites, and comparatively PMMA/$CaCO_3$ nanocomposites have more percentage increase in T_d than PS/$CaCO_3$ nanocomposites. The results attributed a strong interaction between the polymer chains and inorganic particles and consequently preventing

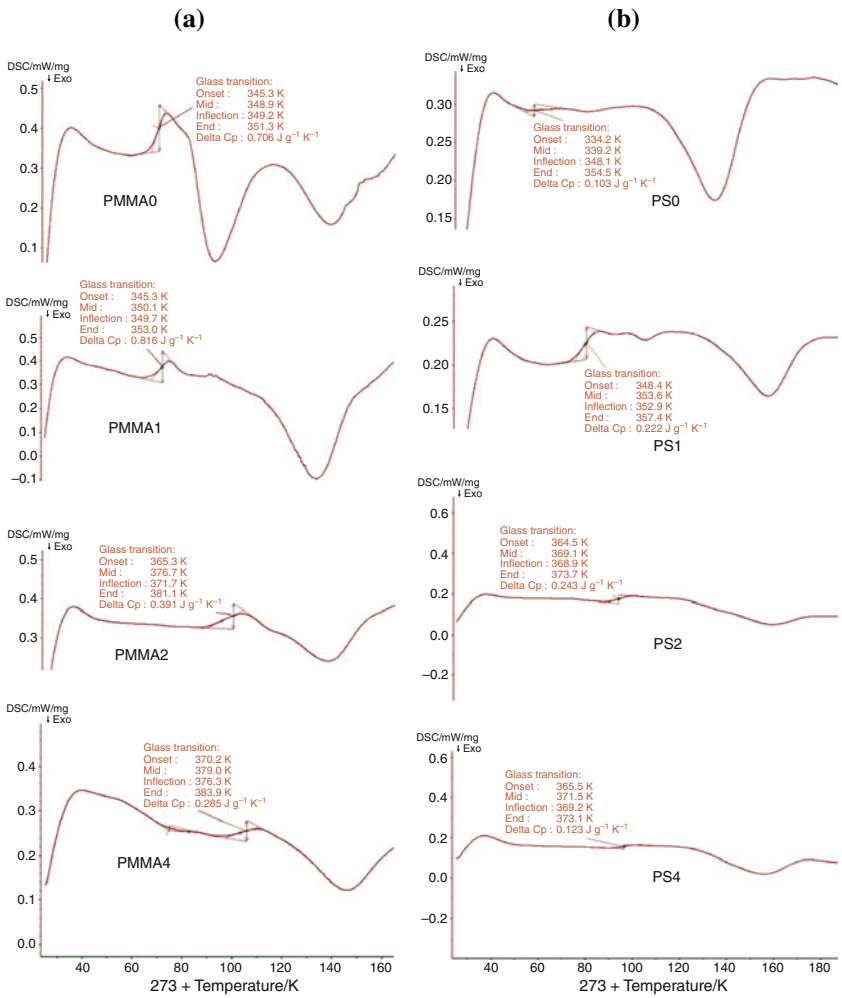

Fig. 6 DSC curve (exothermic peak) of **a** pure PMMA and PMMA/$CaCO_3$ nanocomposites and **b** pure PS and PS/$CaCO_3$ nanocomposites

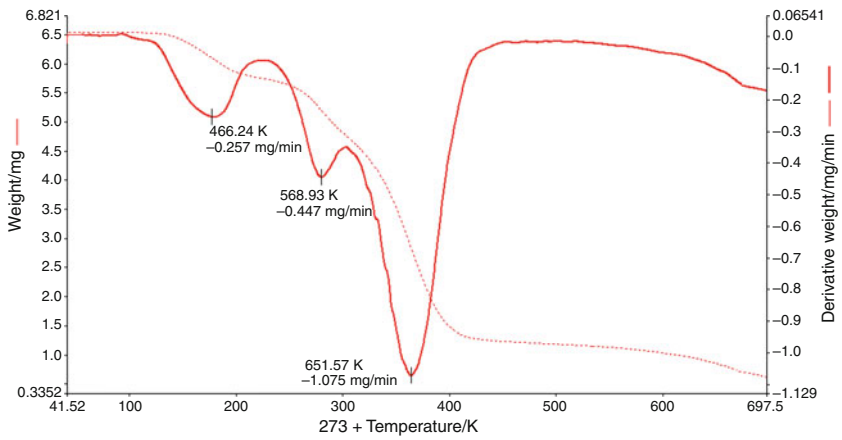

Fig. 7 TG/DTG curve of pure PMMA (PMMA0)

thermal degradation of PMMA and PS polymer matrix. The results show that by the addition of $CaCO_3$ nanoparticles in PMMA and PS polymer matrix, the T_d of these pure polymers were shifted towards higher values in comparison with other nanofillers such as Al_2O_3, ZnO [34], and clay [35].

UV-shielding properties of PMMA/$CaCO_3$ and PS/$CaCO_3$ nanocomposites

Figures 15 and 16 present the UV–Visible absorbance of PMMA/$CaCO_3$ and PS/$CaCO_3$ nanocomposites, respectively. The UV absorbance intensity increased as the

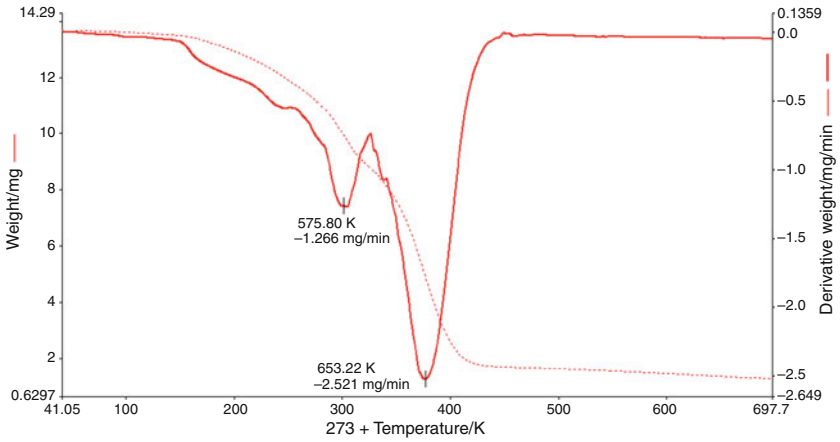

Fig. 8 TG/DTG curve of nanocomposites (PMMA1)

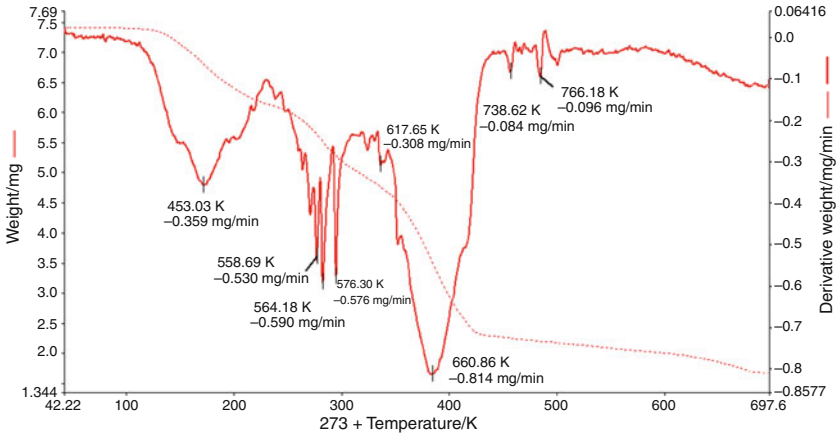

Fig. 9 TG/DTG curve of nanocomposites (PMMA2)

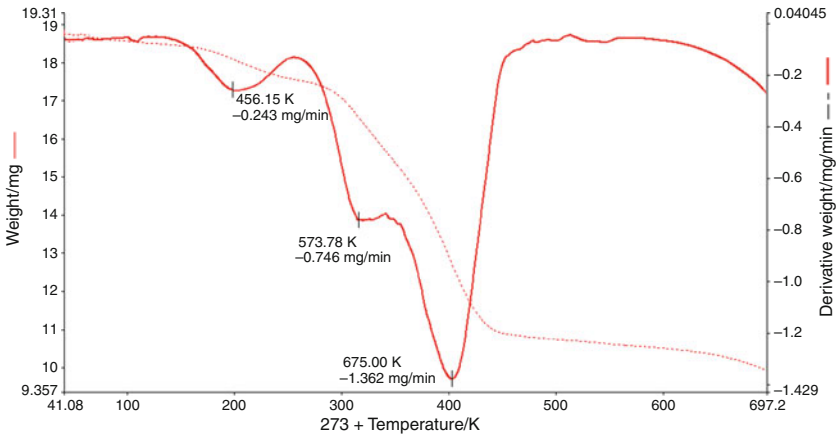

Fig. 10 TG/DTG curve of nanocomposites (PMMA4)

nanoparticles wt% increased. The absorption peak appeared at 335 nm for PMMA/$CaCO_3$ nanocomposites and about 355 nm for PS/$CaCO_3$ nanocomposites. The intensity of this absorbance peak increases with nanoparticles content, and energy band gap of $CaCO_3$ nanoparticles ($\sim$5 eV) [36] was decreased to $\sim$3.7 eV in PMMA/$CaCO_3$ and $\sim$3.5 eV in case of PS/$CaCO_3$ nanocomposites. There was least UV absorbance in both pure polymers, and the absorbance intensity of PS/$CaCO_3$ was greater than the PMMA/$CaCO_3$ nanocomposites. This optical change is caused by a quantum effect of the nanoparticles when size of particles is reduced to a nanoscale [37–39], and adding $CaCO_3$ in polymer matrices may cause the localized states of different colour

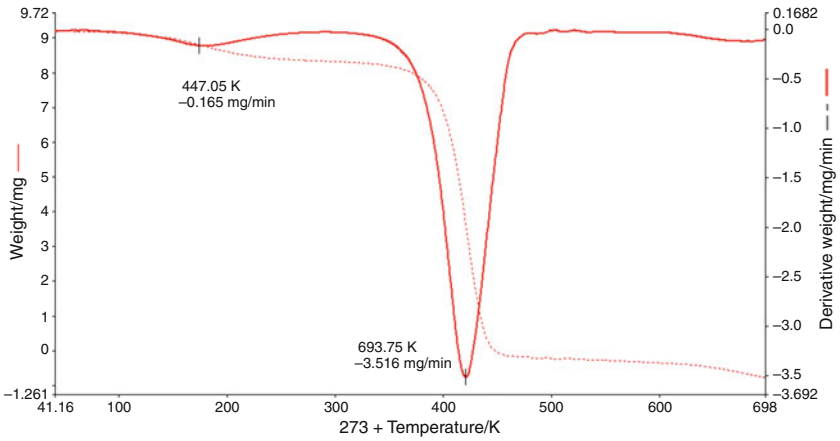

Fig. 11 TG/DTG curve of pure PS (PS0)

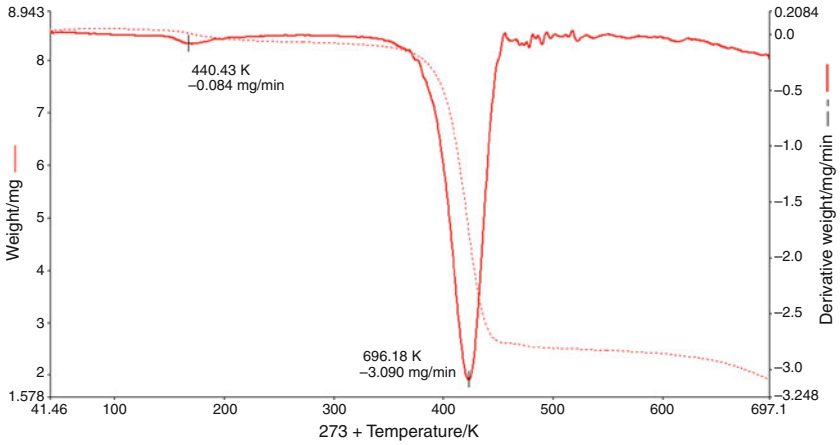

Fig. 12 TG/DTG curve of nanocomposites (PS1)

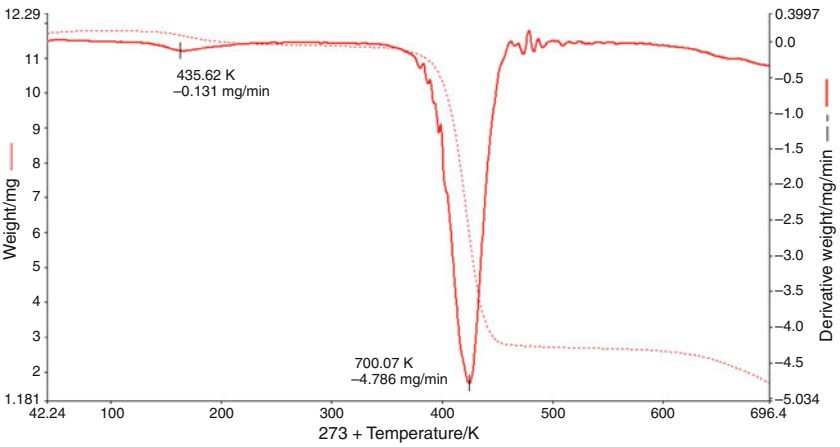

Fig. 13 TG/DTG curve of nanocomposites (PS2)

centers to overlap and extend in the mobility gap. This overlap may give us evidence for decreasing energy gap with the addition of nanosized $CaCO_3$ in the polymer matrix. The nanocomposites thus prepared can protect against UV light. From these results, it can be predicted that PS/$CaCO_3$ nanocomposites have better UV-shielding property as compared to PMMA/$CaCO_3$ nanocomposites. This means that these nanocomposites can improve the weatherability of the polymer film and the undercoats. As a result, it can be potentially applied to UV-shielding materials such as fibers, coating, cosmetics, plastics etc.

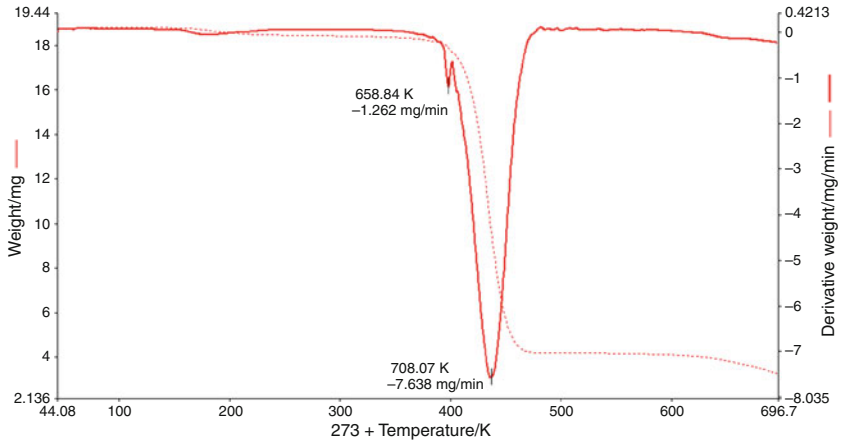

Fig. 14 TG/DTG curve of nanocomposites (PS4)

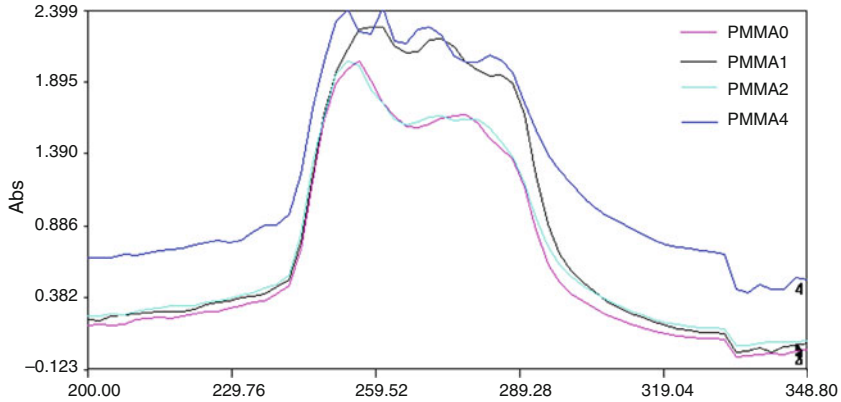

Fig. 15 The UV absorbance of the PMMA/$CaCO_3$ nanocomposites

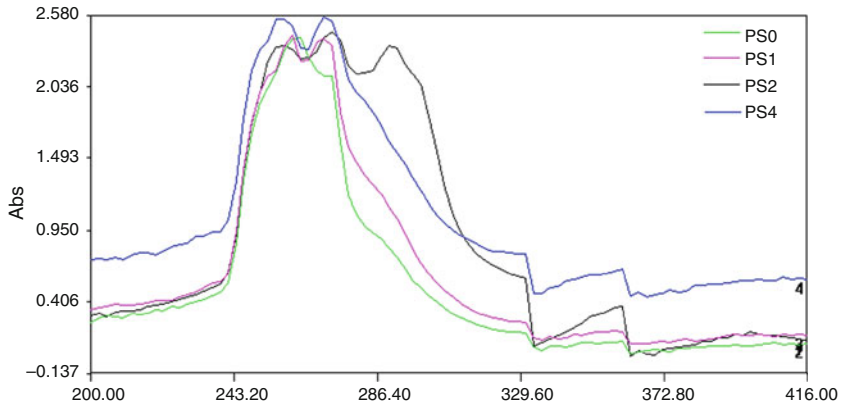

Fig. 16 The UV absorbance of the PS/$CaCO_3$ nanocomposites

Conclusions

Polymer nanocomposites of PMMA and PS containing $CaCO_3$ nanoparticles were prepared by varying the concentration of nanoparticles with respect to polymer matrix through solution mixing technique. The nanoparticles of $CaCO_3$ were successfully synthesized using in situ deposition technique, and the particles size was obtained in the range of 32–35 nm confirmed by XRD and SEM techniques. FT-IR spectral measurements concluded that polymer nanocomposites were formed and also there was intermolecular interaction between the polymers (PMMA and PS) and $CaCO_3$ nanoparticles. SEM results show the dispersion of nanoparticles into the polymer matrixes, and EDS results revealed that the removal of calcium electrons on to the surface of nanocomposite film was very hard as compared to pure $CaCO_3$ nanoparticles, so it was further confirmed that there would interaction between polymer

matrix and nanoparticles. The thermal properties of PMMA/$CaCO_3$ and PS/$CaCO_3$ nanocomposites were marginally higher than respective pure polymer. Further more, the increment in T_g of PS/$CaCO_3$ nanocomposites was higher than PMMA/$CaCO_3$ nanocomposites, but increment in T_d of PS/$CaCO_3$ nanocomposites was less than PMMA/$CaCO_3$ nanocomposites with increase in nanoparticles content because the interaction between polymers and nanoparticles which was in good concurrence with the FT-IR and SEM analysis. The prepared nanocomposites have better UV protection than respective pure polymers. So, this study can be exploited for the commercialization in the case of polymer with higher thermal and better UV protection materials.

Acknowledgements This research study was supported by University Grant Commission, New Delhi (India) Authors also thanks to Dr. R. K. S. Dhakarey, Professor and Dr. Ajay Taneja, Head, Department of Chemistry, Dr. B. R. Ambedkar University, Agra (India), Director, STIC (SAIF) Kochi and IIT Chennai (SAIF) Chennai for providing FT-IR, XRD, DSC, TG/DTG, SEM, and EDS characterization facilities.

References

1. Vodnik VV, Vukovic JV, Nedeljkovic JM. Synthesis and characterization of silver–poly(methyl methacrylate) nanocomposites. Colloid Polym Sci. 2009;287:847–51.
2. Gowri VS, Almeida L, de Amorim MTP, Pacheco NC, Souto AP, Esteves MF, Sanghi SK. Functional finishing of polyamide fabrics using ZnO–PMMA nanocomposites. J Mater Sci. 2010;45:2427–35.
3. Tang F, Cheng G, Pang X, Ma X, Xing F. Synthesis of nano-ZnO/poly(methyl methacrylate) composite microsphere through emulsion polymerization and its UV-shielding property. Colloid Polym Sci. 2006;284:422–8.
4. Wang H, Peng X, Meng S, Zhong W, Du W, Du Q. Poly(methyl methacrylate)/silica/titania ternary nanocomposites with greatly improved thermal and ultraviolet-shielding properties. Polym Degrad Stab. 2006;91:1455–61.
5. Zeng XF, Wang WY, Wang GQ, Chen JF. Influence of the diameter of $CaCO_3$ particles on the mechanical and rheological properties of PVC composites. J Mater Sci. 2008;43:3505–9.
6. Hill J, Orr J, Dunne N. In vitro study investigating the mechanical properties of acrylic bone cement containing calcium carbonate nanoparticles. J Mater Sci Mater Med. 2008;19:3327–33.
7. Ma X, Zhou B, Deng Y, Sheng Y, Wang C, Pen Y, Wang Z. Study on $CaCO_3$/PMMA nanocomposites microsphere by soapless emulsion polymerization. Colloids Surf A: Physicochem Eng Aspects. 2008;312:190–4.
8. Koo JH. Polymer nanocomposites: processing, characterization and applications. New York: McGraw-Hill; 2006.
9. Mann S, Heywood BR, Rajam S, Birchall JD. Controlled crystallization of $CaCO_3$ under stearic acid monolayers. Nature. 1988;334:692–5.
10. Hari B, Ding XF, Guo YP, Deng YH, Wang CY, Li MG, Wang ZC. Multigram scale synthesis and characterization of monodispersed cubic calcium carbonate nanoparticles. J Mater Lett. 2006;60:1515–8.
11. Wei H, Shen Q, Zhao Y, Zhao Y, Wang DJ, Xu DF. Crystallization habit of calcium carbonate in the presence of sodium dodecyl sulfate and or polypyrrolidone. J Cryst Growth. 2004;26:511–6.
12. Ueno Y, Futagawa H, Takagi Y, Ueno A, Mizushima Y. Control of crystal nucleation and growth of calcium carbonate by synthetic substrates. J Controlled Release. 2005;103:93–8.
13. Wang X, Tong W, Li W, Huang H, Yang J, Li G. Preparation and properties of nanocomposites of poly(phenylene sulfide)/calcium carbonate. Polym Bull. 2006;57:953–62.
14. Wang Y, Shen H, Li G, Mai K. Crystallization and melting behavior of PP/$CaCO_3$ nanocomposites during thermo-oxidative degradation. J Therm Anal Calorim. 2010;100:999–1008.
15. Shimpi NG, Mishra S. Synthesis of nanoparticles and its effect on properties of elestomeric nanocomposites. J Nanopart Res. 2010; 12:2093–9.
16. Etienne S, Becker C, Ruch D, Germain A, Calberg C. Synergetic effects of poly(vinyl butryl) and calcium carbonate on thermal stability of poly(vinyl chloride) nanocomposites investigated by TG-FTIR-MS. J Therm Anal Calorim. 2010; 100:667–77.
17. Qing X, Chunfang Z, JianZun Y, Yuan CS. The effects of polymer–nanofiller interaction on the dynamic mechanical properties of PMMA/$CaCO_3$ composites prepared by microemulsion template. J Appl Polym Sci. 2004;91:2739–49.
18. Bose S, Pandey R, Kulkarni MB, Mahanwar PA. Effects of telc and synthetic sodium aluminium silicate (SSAS) on the properties of poly(methyl methacrylate). J Thermoplast Compos Mater. 2005;18:393–405.
19. Ge J, Zeng X, Tao X, Li X, Shen Z, Yun J, Chen J. Preparation and characterization of PS-PMMA/ZnO nanocomposite films with novel properties of high transparency and UV-shielding capacity. J Appl Polym Sci. 2010;118:1507–12.
20. Sun D, Miyatake N, Sue H. Transparent PMMA/ZnO nanocomposite films based on colloidal ZnO quantum dots. Nanotechnology. 2007;18:215–606.
21. Tang E, Liu H, Sun L, Zheng E, Cheng G. Fabrication of zinc oxide/poly(styrene) grafted nanocomposite latex and its dispersion. Eur Polym J. 2007;43:4210–8.
22. Stojanovic D, Oriovic A, Markovic S, Radmilovic V, Uskokovic PS, Aleksic R. Nanosilica/PMMA composites obtained by the modification of silica nanoparticles in a supercritical carbom dioxide–ethanol mixture. J Mater Sci. 2009;44:6223–32.
23. Sun X, Chen X, Liu X, Qu S. Optical properties of poly(methyl methacrylate)-titania nanostructure thin films containing ellipsoid-shaped titania nanoparticles from ex-situ sol-gel method at low growth temperature. Appl Phys B. 2010. doi:10.1007/s00340-010-4265-6.
24. Avella M, Errico ME, Gentile G. PMMA based nanocomposites filled with modified $CaCO_3$ nanoparticles. Macromol Symp. 2007;247:140–6.
25. Ma X, Zhou B, Deng Y, Sheng Y, Wang C, Pen Y, Ma S, Gao Y, Wang Z. Preparation of calcium carbonate/poly(methyl methscarylate) composites microspheres by soapless emulsion polymerization. J Appl Polym Sci. 2009;105:2925–9.
26. Jian-ming S, Yong-zhong B, Zhi-ming H, Zhi-xue W. Preparation of poly(methyl methscarylate)/nanometer calcium carbonate composite by in situ emulsion polymerization. J Zhejiang Uni Sci. 2004;5:709–13.
27. Elimat ZM, Zihlif AM, Avella M. Thermal and optical properties of poly(methyl methacrylate)/calcium carbonate nanocomposites. J Experi Nanosci. 2008;3:259–69.
28. Zeng X, Kong X, Ge J, Liu H, Gao C, Shen Z, Chen J. Effective solution mixing method to fabricate highly transparent and optical functional organic–inorganic nanocomposite film. Ind Eng Chem Res. 2011;50:3253–8.
29. Tu Y, Zhou L, Jin YZ, Gao C, Ye ZZ, Yang YF, Wang QL. Transparent and flexible thin films of ZnO–polystyrene

nanocomposite for UV-shielding applications. J Mater Chem. 2010;20:1594–9.
30. Patil CB, Kapadi UR, Hundiwale DG, Mahulikar PP. Preparation and characterization of poly(vinyl chloride) calcium carbonate nanocoomposites via melt intercation. J Mater Sci. 2009;44: 3118–24.
31. Lysikov AI, Salanov AN, Moroz EM, Okunev AG. Preparation of pure monodisperse calcium carbonate partilces. React Kinet Catal Lett. 2007;90:151–7.
32. White WB. The carbonate minerals. In: Farmer VC, editors. The infrared spectra of minerals. London: Mineralogical Society; 1974.
33. Gaur MS, Rathore BS, Singh PK, Indolia A, Awasthi AM, Bhardwaj S. Thermally stimulated current and differential scanning calorimetry spectroscopy for the study of polymer nanocomposites. J Therm Anal Calorim. 2010;101:315–21.
34. Viratyaporn W, Lehman RL. Effect of nanoparticles on the thermal stability of PMMA nanocomposites prepared by in situ bulk polymerization. J Therm Anal Calorim. 2011;103:267–73.
35. Arora A, Choudhary V, Sharma DK. Effect of clay content and clay/surfactant on the mechanical, thermal and barrier properties of polystyrene/organoclay nanocomposites. J Polym Res. 2010. doi:10.1007/s10965-010-9481-6.
36. Mikheeva OP, Sidorov AI. Optical nonlinearity of wide-bandgap semiconductor and insulator nanoparticles in the visible and near-infrared regions of the spectrum. Tech Phys. 2004;49:739–44.
37. Fujihara S, Naito H, Kimura T. Visible photoluminescence of ZnO nanoparticles dispersed in highly transparent MgF_2 thin-films via sol-gel process. Thin Solid Films. 2001;389:227–32.
38. Nyffenegger RM, Craft B, Shaaban M, Gorer S, Penner RM. A hybrid electrochemical/chemical synthesis of zinc oxide nanoparticles and optically intrinsic thin films. Chem Mater. 1998; 10:1120–9.
39. Wang Y, Herron N. Nanomater-sized semiconductor clusters: materials synthesis, quantum size effects, and photophysical properties. J Phys Chem. 1991;95:525–32.